

Splitting-Particle Methods for Structured Population Models: Convergence and Applications

J. A. Carrillo* P. Gwiazda† A. Ulikowska‡

November 4, 2018

Abstract

We propose a new numerical scheme designed for a wide class of structured population models based on the idea of operator splitting and particle approximations. This scheme is related to the Escalator Boxcar Train (EBT) method commonly used in biology, which is in essence an analogue of particle methods used in physics. Our method exploits the split-up technique, thanks to which the transport step and the nonlocal integral terms in the equation can be separately considered. The order of convergence of the proposed method is obtained in the natural space of finite nonnegative Radon measures equipped with the flat metric. This convergence is studied even adding reconstruction and approximation steps in the particle simulation to keep the number of approximation particles under control. We validate our scheme in several test cases showing the theoretical convergence error. Finally, we use the scheme in situations in which the EBT method does not apply showing the flexibility of this new method to cope with the different terms in general structured population models.

Key words: structured population models, particle method, measure valued solutions, Radon measures, flat metric.

AMS Classification: 92D25, 65M12, 65M75.

1 Introduction

The main purpose of population dynamics models is to describe the evolution of a population, which changes its size, structure, or trait due to birth, growth, death, selection, and mutation processes. Initially, the models are based on linear ordinary differential equations, and as a consequence exponential growing solutions are typically obtained. However, in many cases it is not a realistic phenomenon, since the exponential growth can be inhibited by environmental limitations such as lack of nutrients, space, partners to reproduction, etc. Additionally, these models leave out of consideration the individual's stage of development, which strongly influences its vital functions. For example, fertility and death rates depend heavily on the

*Department of Mathematics, Imperial College London, SW7 2AZ London, United Kingdom. E-mail: carrillo@imperial.ac.uk.

†Institute of Applied Mathematics, Warsaw University. E-mail: pgwiazda@mimuw.edu.pl

‡Institute of Applied Mathematics, Warsaw University. E-mail: aulikowska@mimuw.edu.pl

age of human beings, the process of cell mitosis can be influenced by the age, size or maturity level of the cell, a trait of an offspring may depend on parents traits. Taking into account the population structure usually leads to first order hyperbolic equations. Finally, subsequent generations of individuals produce slight changes in their traits due to small mutations. Selection-mutation models typically lead to nonlocal terms due to the offspring different trait. This paper is devoted to the numerical analysis of such equations written in general as

$$\begin{aligned} \frac{\partial}{\partial t}\mu + \frac{\partial}{\partial x}(b(t, \mu)\mu) + c(t, \mu)\mu &= \int_{\mathbb{R}^+} (\eta(t, \mu))(y) d\mu(y), \\ \mu(0) &= \mu_o, \end{aligned} \quad (1.1)$$

where $t \in [0, T]$ and $x \geq 0$ denote time and a structural variable respectively, b, c, η are vital functions depending on $x \geq 0$, and μ is a Radon measure describing the distribution of individuals with respect to the trait/variable x . The function $b(t, \mu)$ describes the dynamics of the transformation of the individual's state. More precisely, the individual changes its state according to the following ODE

$$\dot{x} = b(t, \mu)(x).$$

By $c(t, \mu)(x)$ we denote a rate of evolution (growth or death rate). The integral on the right hand side accounts for an influx of the new individuals into the system. We assume the following form of the measure-valued function η is of the form

$$\eta(t, \mu)(y) = \sum_{p=1}^r \beta_p(t, \mu)(y) \delta_{x=\bar{x}_p(y)}, \quad (1.2)$$

which means that an individual at the state y gives rise to offspring being at the states $\{\bar{x}_p(y)\}$, $p = 1, \dots, r$. The integral on the right-hand side has to be understood in the Böchner sense, that is, by duality on test functions $\varphi \in \mathbf{C}_0(\mathbb{R}^+)$ functions as

$$\int_{\mathbb{R}^+} \int_{\mathbb{R}^+} \varphi(t, x) [d\eta(t, \mu)(y)](x) d\mu(y) = \sum_{p=1}^r \int_{\mathbb{R}^+} \beta_p(t, \mu)(y) \varphi(\bar{x}_p(y)) d\mu(y). \quad (1.3)$$

In case all new born individuals have the same physiological state x^b , then

$$\eta(t, \mu)(y) = \beta(t, \mu)(y) \delta_{x=x^b}, \quad (1.4)$$

and the integral in (1.3) transforms into a boundary condition. We restrict to integral operators of the form (1.2) for the sake of simplicity. In fact, the continuous dependence of solutions of (1.1) with respect to η in [11] allows for the general case to be approximated by integral operators of the form (1.2), and thus this restriction is done without loss of generality, see Remark 3.23.

In the present paper, we develop a numerical scheme, which is based on results obtained in [13], for the equation (1.1). It turns out that a measure setting used in the latter paper is convenient not only from the analytical but also from the practical numerical simulation viewpoint. Note that the result of a measurement or an observation is usually the number of individuals, whose state is within a specific range. For example, demographic data provide the number of humans within certain age cohorts. A natural way of translating such data into a mathematical language is to make use of Dirac Deltas.

This intuitive idea was the basis for a numerical scheme called the Escalator Boxcar Train (EBT) method developed in [16]. This method approximates in some sense a solution at

time t by a sum of Dirac measures $\sum_{i \in I} m^i(t) \delta_{x^i(t)}$. In the first step, an initial distribution is divided into M cohorts characterized by pairs (m^i, x^i) , for $i = 1, \dots, M$. For the i -th cohort, $m^i(t)$ denotes its weight at time t , which is a number of the individuals within the cohort and $x^i(t)$ is its location at time t , that is, an average value of the structural variable within this cohort. The mass $m^i(t)$ changes its value due to the process of evolution (growth or death), while $x^i(t)$ evolves according to the characteristic lines defined by the transport term. A boundary cohort (m_B, x_B) , that is, the cohort which accounts for the influx of new individuals into the system, evolves in a slightly different way, since its weight changes additionally due to the birth process. Enclosing the boundary cohort into the system, which occurs in certain time moments, is called the internalization process. A power of the described method lies in its simplicity and clear biological meaning of the output. Indeed, integrals of a population's distribution over specified domains, which are the output, are more meaningful than a density's value in nodal points. Originally, the EBT method was designed for equations of the form (1.1) with the most simplified form of the integral kernel (1.4), and since its invention in [16] it has been widely used by biologists, see e.g. [7, 21, 28, 34].

Similar mesh-free methods called particle methods are commonly used in problems, where one has to model a behaviour of large groups of particles or individuals, which interact between each other. Contrary to the EBT, particle methods were originally designed for problems where the number of individuals was preserved and thus the mass conservation law holds. These methods have been successfully used for solving numerically such problems as the Euler equation in fluid mechanics [22, 33] and Vlasov equation in plasma physics [5, 15, 20]. Recently, they are also used in problems related to crowd dynamics and pedestrians flow [31, 30] or collective motion of large groups of agents [19, 12, 25].

As it has been stated above, in structured population models conservation laws do not hold in general. One has to deal with new particles, which appear due to the birth process or mutations. Depending on the model, new individuals may appear only on the boundary or can be distributed over the whole domain. Therefore, one cannot exploit some natural distances for probability measures like Wasserstein distances. The measure approach, which rigorously deals with Dirac Deltas in models coming from biology, is relatively new [23, 24, 11], and thus a convergence of the particle based schemes for these models was difficult to establish for a long period of time. One of the first steps in this direction has been made for the equation (1.1) in [23, 24], where existence, uniqueness, and Lipschitz dependence of solutions on the initial data and model parameters in the space of Radon measures were proved. By the proper choice of a metric authors overcame the nonconservative character of the problem. Namely, they employed a modified Wasserstein distance and the flat metric, known also as the bounded Lipschitz distance. This framework was the theoretical foundations for the very recent proof [6] of the convergence of the EBT method without any explicit error estimates for (1.1)–(1.4).

In this work, we shall explicitly show how the method used for proving the well posedness of (1.1) in [13] can be translated into an applicable numerical scheme. We provide estimates on the order of the convergence for the general models (1.1), covering in particular the case (1.1)–(1.2). The novelty of this paper also concerns the problem of increasing number of Dirac measures that appears due to birth and/or mutation processes. We provide a procedure to construct an approximation of a sum of Dirac Deltas by a smaller amount of deltas, called the measure reconstruction procedure, together with an error of the approximation. This paper is organized as follows. In Section 2, we describe the algorithm and the procedure of a measure

reconstruction. In Section 3, we present the proof of the convergence of the scheme together with the convergence order error analysis. In Section 4, we validate our numerical scheme and implementation by checking the convergence order in some test cases with explicit solutions. We also use this new proposed scheme in several examples to show the flexibility and the accurate approximation of the evolution of the density in structured population models even for long-time asymptotics including cases that are not amenable for the EBT method.

2 Particle Method

2.1 General Description

The main idea of the particle method is to approximate a solution at each time by a sum of Dirac measures. Note that even if the initial data in (1.1) is a sum of Dirac Deltas, the integral term possibly produces a continuous distribution at $t > 0$. This phenomenon can be avoided due to the splitting algorithm, which allows to separate the transport operator from the integral one and simulate the corresponding problems successively. This is essentially the reason why we have exploited this technique in our scheme. To proceed with a description of the method, assume that the approximation of the solution at time $t_k = k\Delta t$ is provided as a sum of Dirac measures, that is,

$$\mu_{t_k} = \sum_{i=1}^{M_k} m_k^i \delta_{x_k^i}, \quad M_k \in \mathbb{N}. \quad (2.1)$$

The procedure of calculating the approximation of the solution at time t_{k+1} is divided into three main steps. In the first step one calculates the characteristic lines for the cohorts (m^i, x^i) given by (2.1), which is equivalent to solving the following ODE's system on a time interval $[t_k, t_{k+1}]$:

$$\frac{d}{ds} x^i(s) = b_k(x^i(s)), \quad x^i(t_k) = x_k^i, \quad i = 1, \dots, M_k, \quad (2.2)$$

where

$$b_k(x) = b(t_k, \mu_{t_k})(x). \quad (2.3)$$

In other words, each Dirac Delta is transported along its characteristic to the new location x_{k+1}^i without changing its mass. The second step consists in creating new Dirac Deltas due to the influx of new individuals and recalculating the mass of each Dirac Delta. We have already mentioned in the introduction above that for each $(t, \nu) \in [0, T] \times \mathcal{M}_+(\mathbb{R}^+)$, η is given by

$$\eta(t, \nu)(y) = \sum_{p=1}^r \beta_p(t, \nu)(y) \delta_{x=\bar{x}_p(y)}. \quad (2.4)$$

From this form of η , it follows that the set of possible new states x_{k+1}^l at time t_k is

$$\{x_{k+1}^l, l = M_k + 1, \dots, M_{k+1}\} := \{\bar{x}_p(x_{k+1}^i), i = 1, \dots, M_k, p = 1, \dots, r\}.$$

Let us define

$$\mu_k^1 = \sum_{i=1}^{M_{k+1}} m_k^i \delta_{x_{k+1}^i},$$

$$c_k(x) = c(t_k, \mu_k^1)(x), \quad (2.5)$$

$$\eta_k(y) = \sum_{p=1}^r \beta_p(t_k, \mu_k^1)(y) \delta_{x=\bar{x}_p(y)} \quad (2.6)$$

and for $i, j \in \{1, \dots, M_{k+1}\}$

$$\alpha(x_{k+1}^i, x_{k+1}^j) = \begin{cases} \beta_p(t_k, \mu_k^1)(x_{k+1}^j), & \text{if } p \text{ is such that } \bar{x}_p(x_{k+1}^j) = x_{k+1}^i, \\ 0, & \text{otherwise.} \end{cases}$$

We cannot solve an ODE system for the masses directly, since new states will be created at any time $t_k < t < t_{k+1}$. Therefore, we approximate it by the following explicit Euler scheme

$$\begin{aligned} \frac{m_{k+1}^i - m_k^i}{t_{k+1} - t_k} &= -c_k(x_{k+1}^i) m_k^i + \sum_{j=1}^{M_{k+1}} \alpha_k(x_{k+1}^i, x_{k+1}^j) m_k^j, \\ m_k^i &= 0, \text{ for } i = M_k + 1, \dots, M_{k+1}. \end{aligned} \quad (2.7)$$

The resulting measure

$$\mu_k^2 = \sum_{i=1}^{M_{k+1}} m_{k+1}^i \delta_{x_{k+1}^i} \quad (2.8)$$

consists of $M_{k+1} \geq M_k$ Dirac Deltas. In some cases, it is necessary to approximate the measure (2.8) by a smaller number of Dirac Deltas (see Subsection 2.3). If so, we define $\mu_{t_{k+1}} = \mathcal{R}(\mu_k^2)$, where $\mathcal{R}(\mu_k^2)$ is the result of this approximation. Otherwise we let $\mu_{t_{k+1}} = \mu_k^2$.

Remark 2.9. *In the particular case where only one new state x^b is allowed, we can use the continuum ODE system:*

$$\begin{aligned} \frac{d}{ds} m^i(s) &= -c_k(x_{k+1}^i) m^i(s), \quad \text{for } i \neq b, \\ \frac{d}{ds} m^b(s) &= -c_k(x^b) m^b(s) + \sum_{j=1}^{M_{k+1}} \alpha_k(x^b, x_{k+1}^j) m^j(s), \end{aligned} \quad (2.10)$$

instead of the Euler approximation (2.7).

In the method presented above, one has to deal with an increasing number of Dirac measures, which is an important issue to solve from the point of view of numerical simulation. In the simplest case that all new individuals have the same size x^b at birth, then just one additional Dirac Delta is created at the boundary at each time step. Unfortunately, in many models the number of new particles increases so fast that after several steps the computational cost become unacceptable. For example, in the case of equation describing the process of cell equal mitosis, the number of Dirac Deltas is doubled at each time step. This growth forces us to approximate the numerical solution by a smaller number of Dirac measures after several iterations. This procedure is called measure reconstruction. We propose some different methods of this reconstruction, which are discussed in the next subsection. In order to rigorously introduce this reconstruction procedure and to discuss the convergence of the particle method above, we first need to introduce several distances between measures which are relevant and useful for those purposes.

2.2 Distances between measures

Through this paper $\mathcal{M}_+(\mathbb{R}^+)$ denotes the space of nonnegative Radon measures with bounded total variation on $\mathbb{R}^+ = \{x \in \mathbb{R} : x \geq 0\}$. We define a metric on $\mathcal{M}_+(\mathbb{R}^+)$ as

$$\rho_F(\mu_1, \mu_2) = \sup \left\{ \int_{\mathbb{R}^+} \varphi \, d(\mu_1 - \mu_2) : \varphi \in \mathbf{C}^1(\mathbb{R}^+; \mathbb{R}) \text{ and } \|\varphi\|_{\mathbf{W}^{1,\infty}} \leq 1 \right\}, \quad (2.11)$$

where $\|\varphi\|_{\mathbf{W}^{1,\infty}} = \max \{ \|\varphi\|_{\mathbf{L}^\infty}, \|\partial_x \varphi\|_{\mathbf{L}^\infty} \}$. ρ_F is known as a *flat metric* or a *bounded Lipschitz distance*. The condition $\mathbf{C}^1(\mathbb{R}^+; \mathbb{R})$ in (2.11) can be replaced by $\mathbf{W}^{1,\infty}(\mathbb{R}^+; \mathbb{R})$ through a standard mollifying sequence argument applied to the test function φ , as its derivative is not involved in the value of the integral, which implies that ρ_F is the metric dual to the $\|\cdot\|_{(\mathbf{W}^{1,\infty})^*}$ distance. Note that in this paper, the space $\mathcal{M}_+(\mathbb{R}^+)$ is equipped with the metric ρ_F and this shall remain until said differently. The space $(\mathcal{M}_+(\mathbb{R}^+), \rho_F)$ is complete and separable.

In the following lemma we introduce ρ related to ρ_F , which turns out to be useful for computational purposes. Since [2, Theorem 6.0.2] gives an explicit formula on the Wasserstein distance between two probability measures in terms of their cumulative distribution functions, we shall exploit this result and relate it to the flat metric. In particular, all error estimates calculated in Section 4 are given in terms of ρ .

Lemma 2.1. *Let $\mu_1, \mu_2 \in \mathcal{M}_+(\mathbb{R}^+)$ be such that $M_{\mu_i} = \int_{\mathbb{R}^+} d\mu_i \neq 0$ and $\tilde{\mu}_i = \mu_i / M_{\mu_i}$ for $i = 1, 2$. Define $\rho : \mathcal{M}_+(\mathbb{R}^+) \times \mathcal{M}_+(\mathbb{R}^+) \rightarrow \mathbb{R}^+$ as the following*

$$\rho(\mu_1, \mu_2) = \min \{ M_{\mu_1}, M_{\mu_2} \} W_1(\tilde{\mu}_1, \tilde{\mu}_2) + |M_{\mu_1} - M_{\mu_2}|, \quad (2.12)$$

where W_1 is the 1-Wasserstein distance. Then, there exists a constant $C_K = \frac{1}{3} \min \left\{ 1, \frac{2}{|K|} \right\}$, such that

$$C_K \rho(\mu_1, \mu_2) \leq \rho_F(\mu_1, \mu_2) \leq \rho(\mu_1, \mu_2),$$

where K is the smallest interval such that $\text{supp}(\mu_1), \text{supp}(\mu_2) \subseteq K$ and $|K|$ is the length of the interval K . If K is unbounded we set $C_K = 0$.

Remark 2.13. *For $\tilde{\mu}_1, \tilde{\mu}_2$ defined as in the lemma above, it holds that*

$$W_1(\tilde{\mu}_1, \tilde{\mu}_2) = \int_0^1 \left| F_{\tilde{\mu}_1}^{-1}(t) - F_{\tilde{\mu}_2}^{-1}(t) \right| dt = \int_{\mathbb{R}^+} |F_{\tilde{\mu}_1}(x) - F_{\tilde{\mu}_2}(x)| dx,$$

which follows from [32, Section 2.2.2]. Since a cumulative distribution function F_μ does not have to be continuous or strictly increasing we set

$$F_\mu^{-1}(s) = \sup \{ x \in \mathbb{R}^+ : F_\mu(x) \leq s \}, s \in [0, 1].$$

Remark 2.14. *Let $\mu \in \mathcal{M}_+(\mathbb{R}^+)$ be a probability measure and $M_1, M_2 > 0$. Then,*

$$\rho_F(M_1\mu, M_2\mu) \leq |M_1 - M_2|. \quad (2.15)$$

Indeed, let $\varphi \in \mathbf{C}^1(\mathbb{R}^+; \mathbb{R})$ be such that $\|\varphi\|_{\mathbf{W}^{1,\infty}} \leq 1$. Then,

$$\int_{\mathbb{R}^+} \varphi(x) \, d(M_1\mu - M_2\mu)(x) \leq |M_1 - M_2| \int_{\mathbb{R}^+} \|\varphi\|_{\mathbf{L}^\infty} \, d\mu(x) \leq |M_1 - M_2|.$$

Taking supremum over all admissible functions φ proves the assertion.

Proof of Lemma 2.1. Let $\mu, \nu \in \mathcal{M}_+(\mathbb{R}^+)$ be probability measures. Assume for the moment that K is bounded, so that $|K| < +\infty$. Note that in the definition of W_1

$$W_1(\mu, \nu) = \sup \left\{ \int_{\mathbb{R}^+} \varphi \, d(\mu - \nu) : \mathbf{Lip}(\varphi) \leq 1 \right\},$$

we can assume without loss of generality that $\|\varphi\|_{\mathbf{L}^\infty} \leq |K|/2$. Indeed, for any φ such that $\mathbf{Lip}(\varphi) \leq 1$, there exists a constant a and a function $\tilde{\varphi}$ such that $\mathbf{Lip}(\tilde{\varphi}) \leq 1$, $\|\tilde{\varphi}\|_{\mathbf{L}^\infty} \leq |K|/2$ and $\varphi = a + \tilde{\varphi}$. Observe that by taking a to be the middle point of the interval K , and taking into account that $\mathbf{Lip}(\tilde{\varphi}) \leq 1$ and the support of the measures is included in K , then $\|\tilde{\varphi}\|_{\mathbf{L}^\infty} \leq |K|/2$ in K . Since the values of φ can be changed arbitrarily outside K , then we can assume that $\|\tilde{\varphi}\|_{\mathbf{L}^\infty} \leq |K|/2$ without loss of generality. As a consequence, we deduce

$$\int_{\mathbb{R}^+} \varphi(x) \, d(\mu - \nu)(x) = a \int_{\mathbb{R}^+} d(\mu - \nu)(x) + \int_{\mathbb{R}^+} \tilde{\varphi}(x) \, d(\mu - \nu)(x) = \int_{\mathbb{R}^+} \tilde{\varphi}(x) \, d(\mu - \nu)(x),$$

since $\int_{\mathbb{R}^+} d(\mu - \nu)(x)$ is equal to zero due to the fact that μ and ν have the same mass. Therefore, we infer that

$$\begin{aligned} W_1(\mu, \nu) &= \sup \left\{ \int_{\mathbb{R}^+} \varphi \, d(\mu - \nu) : \|\varphi\|_{\mathbf{L}^\infty} \leq |K|/2, \mathbf{Lip}(\varphi) \leq 1 \right\} \\ &\leq \sup \left\{ \int_{\mathbb{R}^+} \varphi \, d(\mu - \nu) : \|\varphi\|_{\mathbf{W}^{1,\infty}} \leq \max\{1, |K|/2\} \right\} = \max \left\{ 1, \frac{|K|}{2} \right\} \rho_F(\mu, \nu). \end{aligned}$$

Now, let μ_1, μ_2 be as in the statement of the Lemma. Then,

$$\begin{aligned} \rho_F(\mu_1, \mu_2) &= M_{\mu_1} \rho_F \left(\frac{\mu_1}{M_{\mu_1}}, \frac{\mu_2}{M_{\mu_1}} \right) \leq M_{\mu_1} \rho_F \left(\frac{\mu_1}{M_{\mu_1}}, \frac{\mu_2}{M_{\mu_2}} \right) + M_{\mu_1} \rho_F \left(\frac{\mu_2}{M_{\mu_2}}, \frac{\mu_2}{M_{\mu_1}} \right) \\ &\leq M_{\mu_1} \rho_F(\tilde{\mu}_1, \tilde{\mu}_2) + M_{\mu_1} M_{\mu_2} \left| \frac{1}{M_{\mu_1}} - \frac{1}{M_{\mu_2}} \right| \\ &= M_{\mu_1} W_1(\tilde{\mu}_1, \tilde{\mu}_2) + |M_{\mu_1} - M_{\mu_2}|, \end{aligned}$$

where we used triangle inequality, inequality (2.15) and the fact that $\rho_F(\tilde{\mu}_1, \tilde{\mu}_2) \leq W_1(\tilde{\mu}_1, \tilde{\mu}_2)$. Analogously, we obtain

$$\rho_F(\mu_1, \mu_2) \leq M_{\mu_2} W_1(\tilde{\mu}_1, \tilde{\mu}_2) + |M_{\mu_1} - M_{\mu_2}|$$

and thus,

$$\rho_F(\mu_1, \mu_2) \leq \min \{M_{\mu_1}, M_{\mu_2}\} W_1(\tilde{\mu}_1, \tilde{\mu}_2) + |M_{\mu_1} - M_{\mu_2}| = \rho(\mu_1, \mu_2).$$

Note that this estimate does not depend on $|K|$.

Assume that K is bounded, so that the argument above applies. Using $\varphi = \pm 1$ as a test function in (2.11), we obtain that $|M_{\mu_1} - M_{\mu_2}| \leq \rho_F(\mu_1, \mu_2)$. Then,

$$\begin{aligned} \rho(\mu_1, \mu_2) &\leq M_{\mu_1} W_1(\tilde{\mu}_1, \tilde{\mu}_2) + |M_{\mu_1} - M_{\mu_2}| \\ &= M_{\mu_1} \max\{1, |K|/2\} \rho_F(\tilde{\mu}_1, \tilde{\mu}_2) + |M_{\mu_1} - M_{\mu_2}| \\ &\leq \max\{1, |K|/2\} \rho_F \left(\mu_1, \frac{M_{\mu_1}}{M_{\mu_2}} \mu_2 \right) + \rho_F(\mu_1, \mu_2) \end{aligned}$$

$$\begin{aligned}
&\leq \max\{1, |K|/2\} \left(\rho_F(\mu_1, \mu_2) + \rho_F\left(\mu_2, \frac{M_{\mu_1}}{M_{\mu_2}} \mu_2\right) \right) + \rho_F(\mu_1, \mu_2) \\
&\leq 2 \max\{1, |K|/2\} \rho_F(\mu_1, \mu_2) + \max\{1, |K|/2\} M_{\mu_2} \left| 1 - \frac{M_{\mu_1}}{M_{\mu_2}} \right| \\
&\leq 3 \max\{1, |K|/2\} \rho_F(\mu_1, \mu_2),
\end{aligned}$$

which implies that

$$\frac{1}{3} \min\left\{1, \frac{2}{|K|}\right\} \rho(\mu_1, \mu_2) \leq \rho_F(\mu_1, \mu_2).$$

In case $|K| = +\infty$ we set $C_K = 0$ obtaining a trivial inequality $0 \leq \rho_F(\mu_1, \mu_2)$. \square

Remark 2.16. *The dependence of the constant C_K on a length of the interval K express a small sensitivity of the flat metric in the case where a distance between supports of measures is large. In particular, the flat distance for two Dirac measures $\delta_{x=a}$ and $\delta_{x=b}$ is equal to*

$$\rho_F(\delta_{x=a}, \delta_{x=b}) = \min\{2, |a - b|\}.$$

Now, we can precisely discuss the measure reconstruction by approximation with a fixed number of particles of continuum or larger number of particles distributions.

2.3 Measure Reconstruction

Due to Lemma 2.1, we restrict our analysis to probability measures. Let $\mu = \sum_{i=1}^M m_i \delta_{x_i}$ be a probability measure with a compact support $K = [k_1, k_2]$. The aim of the reconstruction is to find a smaller number of Dirac Deltas $\bar{M} < M$ such that

$$\mathcal{R}_o(\mu) := \operatorname{argmin} W_1 \left(\mu, \sum_{j=1}^{\bar{M}} n_j \delta_{y_j} \right), \quad \text{where } \sum_{j=1}^{\bar{M}} n_j = 1 \text{ and } n_j \geq 0, y_j \in \mathbb{R}^+.$$

This minimisation procedure is essentially a linear programming problem which, under some particular assumptions on cycles, can be solved by the simplex algorithm providing the global minimum. This choice is the optimal for the reconstruction procedure. However, its complexity is at least cubic. From that reason, we exploit less costly (linear cost in the size of the problem) methods of reconstruction, which provide the error of the order $\mathcal{O}(1/\bar{M})$. Note that the cubic cost is unacceptable in our case, since the total cost of the method is quadratic if the number of particles grows linearly with the time step.

A) Fixed-location reconstruction: The idea of the fixed-location reconstruction is to divide the support of the measure μ into \bar{M} equal intervals and put a Dirac Delta with a proper mass in the middle of each interval. The mass of this Dirac Delta is equal to the mass of μ contained in this particular interval. Let $\Delta x = |K|/\bar{M}$ and define

$$\tilde{x}_j = k_1 + \left(j - \frac{1}{2}\right) \Delta x, \quad \tilde{m}_j = \begin{cases} \mu\left([\tilde{x}_j - \Delta x/2, \tilde{x}_j + \Delta x/2]\right), & \text{for } j = 1, \dots, \bar{M} - 1, \\ \mu\left([\tilde{x}_{\bar{M}} - \Delta x/2, \tilde{x}_{\bar{M}} + \Delta x/2]\right), & \text{for } j = \bar{M}, \end{cases}$$

and

$$\mathcal{R}_l(\mu) := \sum_{j=1}^{\bar{M}} \tilde{m}_j \delta_{\tilde{x}_j}.$$

To estimate the error between μ and $\mathcal{R}_l(\mu)$ consider a transportation plan γ between both measures. Then, according to [32, Introduction], we have

$$W_1(\mu, \mathcal{R}_l(\mu)) \leq \int_{\mathbb{R}_+^2} |x - y| d\gamma(x, y) \leq \int_{\mathbb{R}_+^2} \frac{\Delta x}{2} d\gamma(x, y) \leq \frac{\Delta x}{2} = \frac{|K|}{2\bar{M}}. \quad (2.17)$$

The second inequality follows from the fact that each particle was shifted by a distance not greater than a half of the interval of a length Δx , while the third one is a consequence of the fact that γ is a probability measure on \mathbb{R}_+^2 .

B) Fixed-Equal mass reconstruction: The aim of the fixed-equal mass reconstruction is to distribute Dirac Deltas of equal masses over the support of a given measure in a proper way. In our particular case, we want to reduce the number of Dirac Deltas from M to \bar{M} , and thus we need to explain an algorithm allowing for splitting of the Dirac Deltas into two. The definition of the reconstruction operator $\mathcal{R}_m(\mu)$ is as follows: we set

$$\tilde{m}_j = \frac{1}{\bar{M}}, \text{ for } j = 1, \dots, \bar{M}.$$

The scheme for determining \tilde{x}_j is the following. We first look for an index n_1 , such that

$$\sum_{i=1}^{n_1-1} m_i < \frac{1}{\bar{M}} \leq \sum_{i=1}^{n_1} m_i.$$

We set

$$\tilde{x}_1 = \sum_{i=1}^{n_1-1} m_i x_i + m'_{n_1} x_{n_1}, \text{ where } m'_{n_1} = \frac{1}{\bar{M}} - \sum_{i=1}^{n_1-1} m_i x_i.$$

Namely, the mass located in x_{n_1} is split into two parts – the amount of mass equal to m'_{n_1} is shifted to \tilde{x}_1 and the rest, that is, $m_{n_1} - m'_{n_1}$ stays in x_{n_1} . For simplicity, we redefine $m_{n_1} := m_{n_1} - m'_{n_1}$ and repeat the procedure described above until the last point $\tilde{x}_{\bar{M}}$ is found to get the final form of the reconstruction

$$\mathcal{R}_m(\mu) := \sum_{j=1}^{\bar{M}} \tilde{m}_j \delta_{\tilde{x}_j}.$$

Note that in each step of the procedure one changes the locations of the Dirac Deltas, of which joint mass is not greater than m . Using an analogous argument as in the previous case, we conclude that in the j -th step we commit an error not greater than $|x_{n_j} - x_{n_{j-1}}|m$, where $x_{n_o} = k_1$. Since $k_1 = x_{n_o} \leq x_{n_1} \cdots \leq x_{n_{\bar{M}}} \leq k_2$, the total error can be bounded by

$$W_1(\mu, \mathcal{R}_m(\mu)) \leq \frac{|K|}{\bar{M}}. \quad (2.18)$$

The findings above can be summarized in the following

Corollary 2.2. *The error of the fixed-location $\mathcal{R}_l(\mu)$ and fixed-equal mass $\mathcal{R}_m(\mu)$ reconstructions is of the order of $\mathcal{O}(1/\bar{M})$ where \bar{M} is the number of Dirac Deltas approximating the original measure μ .*

These reconstructions can be used at $t = 0$, if the initial data in (1.1) is not a sum of Dirac Deltas or at $t > 0$ in order to deal with the problem of increasing number of Dirac Deltas, which are produced due to birth and/or mutation processes. We introduce the following notation:

- $E_I(\bar{M}_o)$ is the upper bound for the error of the initial data reconstruction defined in terms of W_1 distance. More specifically, for a measure μ such that $M_\mu := \int_{\mathbb{R}^+} d\mu(x) > 0$, it holds that

$$W_1\left(\frac{\mu}{M_\mu}, \frac{\mathcal{R}(\mu)}{M_\mu}\right) \leq E_I(\bar{M}_o).$$

Here, the reconstruction operator $\mathcal{R}(\mu)$ refers to either $\mathcal{R}_l(\mu)$ or $\mathcal{R}_m(\mu)$.

- $E_R(\bar{M})$ is the upper bound for the error of the measure reconstruction at time $t > 0$ defined in terms of W_1 distance as above.

We are now ready to state and prove the main convergence result.

3 Convergence Results

3.1 Assumptions and theoretical results on splitting

For the sake of the reader, we recall the theoretical results on splitting for the equation (1.1) obtained in [13]. The assumptions on the parameter functions b, c and β_p , $p = 1, \dots, r$, are the following

$$b, c, \beta_p : [0, T] \times \mathcal{M}^+(\mathbb{R}^+) \rightarrow \mathbf{W}^{1,\infty}(\mathbb{R}^+; \mathbb{R}), \quad (3.1)$$

$$\bar{x}_p : \mathbb{R}^+ \rightarrow \mathbb{R}^+, \quad (3.2)$$

where $b(t, \mu)(0) \geq 0$ for $(t, \mu) \in [0, T] \times \mathcal{M}^+(\mathbb{R}^+)$ and $p = 1, \dots, r$. We require the following regularity

$$b, c, \beta_p \in \mathbf{BC}^{\alpha,1}\left([0, T] \times \mathcal{M}^+(\mathbb{R}^+); \mathbf{W}^{1,\infty}(\mathbb{R}^+; \mathbb{R})\right), \quad (3.3)$$

$$\bar{x}_p \in \mathbf{Lip}(\mathbb{R}^+; \mathbb{R}^+). \quad (3.4)$$

Here, $\mathbf{BC}^{\alpha,1}([0, T] \times \mathcal{M}^+(\mathbb{R}^+); \mathbf{W}^{1,\infty}(\mathbb{R}^+; \mathbb{R}))$ is the space of $\mathbf{W}^{1,\infty}(\mathbb{R}^+; \mathbb{R})$ valued functions which are bounded in the $\|\cdot\|_{\mathbf{W}^{1,\infty}}$ norm, Hölder continuous with exponent $0 < \alpha \leq 1$ with respect to time and Lipschitz continuous in ρ_F with respect to the measure variable. This space is equipped with the $\|\cdot\|_{\mathbf{BC}^{\alpha,1}}$ norm defined by

$$\|f\|_{\mathbf{BC}^{\alpha,1}} = \sup_{t \in [0, T], \mu \in \mathcal{M}^+(\mathbb{R}^+)} \left(\|f(t, \mu)\|_{\mathbf{W}^{1,\infty}} + \mathbf{Lip}(f(t, \cdot)) + H_\alpha(f(\cdot, \mu)) \right), \quad (3.5)$$

where $\mathbf{Lip}(f)$ is the Lipschitz constant of a function f and

$$H_\alpha(f(\cdot, \mu)) := \sup_{s_1, s_2 \in [0, T]} \frac{\|f(s_1, \mu) - f(s_2, \mu)\|_{\mathbf{W}^{1,\infty}}}{|s_1 - s_2|^\alpha}.$$

For any $f \in \mathbf{BC}^{\alpha,1}([0, T] \times \mathcal{M}^+(\mathbb{R}^+); \mathbf{W}^{1,\infty}(\mathbb{R}^+; \mathbb{R}))$ and any $\mu : [0, T] \rightarrow \mathcal{M}^+(\mathbb{R}^+)$, we define

$$\|f\|_{\mathbf{BC}} = \sup_{t \in [0, T]} \|f(t, \mu(t))\|_{\mathbf{L}^\infty}.$$

Regularity of β_p and x_p imposed in (3.1)–(3.4) guarantees that η defined by (1.2) fulfills the assumptions of [13, Theorem 2.11] and thus, (1.1) is well posed. We recall this result next.

Theorem 3.1. *Let (3.1)–(3.4) hold. Then, there exists a unique solution*

$$\mu \in (\mathbf{BC} \cap \mathbf{Lip})([0, T]; \mathcal{M}^+(\mathbb{R}^+))$$

to (1.1). Moreover, the following properties are satisfied:

i) For all $0 \leq t_1 \leq t_2 \leq T$ there exist constants K_1 and K_2 , such that

$$\rho_F(\mu(t_1), \mu(t_2)) \leq K_1 e^{K_2(t_2-t_1)} \mu_o(\mathbb{R}^+)(t_2 - t_1).$$

ii) Let $\mu_1(0), \mu_2(0) \in \mathcal{M}^+(\mathbb{R}^+)$ and $b_i, c_i, \beta_i = (\beta_1^i, \dots, \beta_r^i)$ satisfy assumptions (3.1) - (3.4) for $i = 1, 2, p = 1, \dots, r$. Let μ_i solve (1.1) with initial datum $\mu_i(0)$ and coefficients (b_i, c_i, β_i) . Then, there exist constants C_1, C_2 and C_3 such that for all $t \in [0, T]$

$$\rho_F(\mu_1(t), \mu_2(t)) \leq e^{C_1 t} \rho_F(\mu_1(0), \mu_2(0)) + C_2 e^{C_3 t} t \|(b_1, c_1, \beta_1) - (b_2, c_2, \beta_2)\|_{\mathbf{BC}}.$$

where

$$\|(b, c, \beta)\|_{\mathbf{BC}} = \|b\|_{\mathbf{BC}} + \|c\|_{\mathbf{BC}} + \sum_{p=1}^r \|\beta_p\|_{\mathbf{BC}}.$$

3.2 Error estimates in ρ_F

The aim of this subsection is to obtain an estimate on the error between the numerical solution μ_t and the exact solution $\mu(t)$. Let $[0, T]$ be a time interval, N be a number of time steps, $\Delta t = T/N$ be the time step. We define the time mesh $\{t_k\}_{k=0}^N$, where $t_k = k\Delta t$. Let $\bar{M}_k, k = 0, 1, \dots, N$, be parameters of the measure reconstruction. In particular, \bar{M}_o is the number of Dirac Deltas approximating the initial condition and \bar{M}_k stands for the number of Dirac measures approximating the numerical solution at $t > 0$ after a reconstruction, if performed. We assume that reconstructions are done every n steps, which means that there are $\mathcal{K} = N/n$ reconstructions, each at time t_{jn} , where $j = 1, \dots, \mathcal{K}$. Let \bar{M} be the number of Dirac Deltas after the reconstruction that will not depend on time.

Theorem 3.2. *Let μ be a solution to (1.1) with initial data μ_o . Assume that μ_{t_m} is defined by the numerical scheme described in Subsection 2.1 and $m = jn$ for some $j \in \{1, \dots, \mathcal{K}\}$, i.e., that t_m is the time after j reconstructions. Then, there exists C depending only on the parameter functions, the initial data, and T such that*

$$\rho_F(\mu_{t_m}, \mu(t_m)) \leq C (\Delta t + (\Delta t)^\alpha + E_I(\bar{M}_o) + E_R(\bar{M})j). \quad (3.6)$$

Remark 3.7. *The error estimate (3.6) accounts for different error sources. More specifically, the error of the order $\mathcal{O}(\Delta t)$ is a consequence of the splitting algorithm. The term of order $\mathcal{O}((\Delta t)^\alpha)$ follows from the fact that we solve (2.2)–(2.7) with parameter functions independent of time, while b, c and η are in fact of \mathbf{C}^α regularity with respect to time. Finally, E_I and E_R*

are the errors coming from the measure reconstruction procedure that are of the order $1/\bar{M}_o$ and $1/\bar{M}$ respectively as proven in subsection 2.3. Thinking about $1/\bar{M}$, with $\bar{M} = \bar{M}_o$, as the spatial discretization Δx and for $\alpha = 1$, we obtain that the method is of order one both in space and in time.

Proof of Theorem 3.2. The proof is divided into several steps. For simplicity, in all estimates below, we will use a generic constant C , without specifying its exact form that may change from line to line.

Step 1: The auxiliary scheme. Let us define the auxiliary semi-continuous scheme, which consists in solving subsequently the following problems:

$$\begin{cases} \partial_t \mu + \partial_x(\bar{b}_k(x)\mu) = 0, & \text{on } [t_k, t_{k+1}] \times \mathbb{R}^+, \\ \mu(t_k) = \bar{\mu}_k \end{cases} \quad (3.8)$$

and

$$\begin{cases} \partial_t \mu = -\bar{c}_k(x)\mu + \int_{\mathbb{R}^+} \bar{\eta}_k(y) d\mu(y), & \text{on } [t_k, t_{k+1}] \times \mathbb{R}^+, \\ \mu(t_k) = \bar{\mu}_k^1, \end{cases} \quad (3.9)$$

where $\bar{\mu}_k \in \mathcal{M}^+(\mathbb{R}^+)$, $\bar{\mu}_k^1$ is the solution to (3.8) at time t_{k+1} and \bar{b}_k , \bar{c}_k , and $\bar{\eta}_k$ are defined as

$$\bar{b}_k(x) = b(t_k, \bar{\mu}_k)(x), \quad (3.10)$$

$$\bar{c}_k(x) = c(t_k, \bar{\mu}_k^1), \quad \bar{\eta}_k(y) = \sum_{p=1}^r \beta_p(t_k, \bar{\mu}_k^1)(y) \delta_{x=\bar{x}_p(y)}.$$

A solution to the second equation at time t_{k+1} is denoted by $\bar{\mu}_k^2$. The output of one time step of our scheme is defined as $\bar{\mu}_{k+1} = \mathcal{R}(\bar{\mu}_k^2)$.

Step 2: Error of the reconstruction. Since $\bar{\mu}_{k+1}$ arises from $\bar{\mu}_k^2$ through the reconstruction, masses of both measures are equal. Therefore, application of Lemma 2.1 yields

$$\rho_F(\bar{\mu}_{k+1}, \bar{\mu}_k^2) \leq \rho(\bar{\mu}_{k+1}, \bar{\mu}_k^2) = M_{\bar{\mu}_k^2} W_1 \left(\frac{\bar{\mu}_{k+1}}{M_{\bar{\mu}_k^2}}, \frac{\bar{\mu}_k^2}{M_{\bar{\mu}_k^2}} \right) \leq M_{\bar{\mu}_k^2} E_R(\bar{M}), \quad (3.11)$$

where $M_{\bar{\mu}_k^2} = \bar{\mu}_{k+1}(\mathbb{R}^+) = \bar{\mu}_k^2(\mathbb{R}^+)$ and $E_R(\bar{M})$ is the error of the reconstruction introduced in Subsection 2.3. As stated in Corollary 2.2, $E_R(\bar{M})$ is of order $1/\bar{M}$ for both reconstructions. Note that $M_{\bar{\mu}_k^2}$ can be bounded independently on k . Indeed, on each time interval $[t_k, t_{k+1}]$ mass grows at most exponentially, which follows from [13, Theorem 2.10, (i)], and reconstructions, if performed, do not change the mass. Thus, there exists a constant $C = C(T, b, c, \eta, \mu_o)$ such that $M_{\bar{\mu}_k^2} \leq C$.

Step 3: Error of splitting. Let $\nu(t)$ be a solution to (1.1) on a time interval $[t_k, t_{k+1}]$ with initial datum $\bar{\mu}_k$ and parameter functions \bar{b}_k , \bar{c}_k , $\bar{\eta}_k$, where \bar{b}_k is defined by (3.10),

$$\bar{c}_k(x) = c(t_k, \bar{\mu}_k), \quad (3.12)$$

$$\bar{\eta}_k(y) = \sum_{p=1}^r \bar{\beta}_{p,k}(y) \delta_{x=\bar{x}_p(y)}, \quad \text{where } \bar{\beta}_{p,k}(y) = \beta_p(t_k, \bar{\mu}_k)(y). \quad (3.13)$$

According to [14, Proposition 2.7] and [13, Proposition 2.7], the distance between $\bar{\mu}_k^2$ and $\nu(t_{k+1})$, that is, the error coming from the application of the splitting algorithm can be estimated as

$$\rho_F(\bar{\mu}_k^2, \nu(t_{k+1})) \leq C(\Delta t)^2. \quad (3.14)$$

To estimate a distance between $\nu(t_{k+1})$ and $\mu(t_{k+1})$ consider $\zeta(t)$, which is a solution to (1.1) on a time interval $[t_k, t_{k+1}]$ with initial data $\mu(t_k)$ and coefficients $\bar{b}_k, \bar{c}_k, \bar{\eta}_k$. By triangle inequality

$$\rho_F(\nu(t_{k+1}), \mu(t_{k+1})) \leq \rho_F(\nu(t_{k+1}), \zeta(t_{k+1})) + \rho_F(\zeta(t_{k+1}), \mu(t_{k+1})).$$

The first term of the inequality above is a distance between solutions to (1.1) with different initial data, that is, $\bar{\mu}_k$ and $\mu(t_k)$ respectively. The second term is equal to a distance between solutions to (1.1) with coefficients $(\bar{b}_k, \bar{c}_k, \bar{\eta}_k)$ defined by (3.10), (3.12), and (3.13), and $(b(t, \mu(t)), c(t, \mu(t)), \eta(t, \mu(t)))$. By the continuity of solutions to (1.1) with respect to the initial datum and coefficients in Theorem 3.1, we obtain

$$\rho_F(\nu(t_{k+1}), \zeta(t_{k+1})) \leq e^{C\Delta t} \rho_F(\bar{\mu}_k, \mu(t_k)), \quad (3.15)$$

and

$$\rho_F(\zeta(t_{k+1}), \mu(t_{k+1})) \leq C\Delta t e^{C\Delta t} \left(\|\bar{b}_k - b\|_{\overline{\mathbf{BC}}} + \|\bar{c}_k - c\|_{\overline{\mathbf{BC}}} + \sum_{p=1}^r \|\bar{\beta}_{p,k} - \beta_p\|_{\overline{\mathbf{BC}}} \right), \quad (3.16)$$

where

$$\begin{aligned} \|\bar{b}_k - b\|_{\overline{\mathbf{BC}}} &= \sup_{t \in [t_k, t_{k+1}]} \|\bar{b}_k - b(t, \mu(t))\|_{\mathbf{L}^\infty}, \\ \|\bar{c}_k - c\|_{\overline{\mathbf{BC}}} &= \sup_{t \in [t_k, t_{k+1}]} \|\bar{c}_k - c(t, \mu(t))\|_{\mathbf{L}^\infty}, \end{aligned} \quad (3.17)$$

$$\|\bar{\beta}_{p,k} - \beta_p\|_{\overline{\mathbf{BC}}} = \sup_{t \in [t_k, t_{k+1}]} \|\bar{\beta}_{p,k} - \beta_p(t, \mu(t))\|_{\mathbf{L}^\infty}. \quad (3.18)$$

Due to the assumptions (3.1)–(3.4) and the definition of $\bar{b}_k, \bar{c}_k, \bar{\eta}_k$ we obtain

$$\begin{aligned} \|\bar{b}_k - b(t, \mu(t))\|_{\mathbf{L}^\infty} &\leq \|b(t_k, \bar{\mu}_k) - b(t_k, \mu(t))\|_{\mathbf{L}^\infty} + \|b(t_k, \mu(t)) - b(t, \mu(t))\|_{\mathbf{L}^\infty} \\ &\leq \mathbf{Lip}(b(t_k, \cdot)) \rho_F(\bar{\mu}_k, \mu(t)) + \|b\|_{\mathbf{BC}^{\alpha,1}} |t - t_k|^\alpha \\ &\leq \|b\|_{\mathbf{BC}^{\alpha,1}} [\rho_F(\bar{\mu}_k, \mu(t)) + (\Delta t)^\alpha]. \end{aligned} \quad (3.19)$$

Using Lipschitz continuity of the solution $\mu(t)$, see [13, Theorem 2.11], we obtain

$$\rho_F(\bar{\mu}_k, \mu(t)) \leq \rho_F(\bar{\mu}_k, \mu(t_k)) + \rho_F(\mu(t_k), \mu(t)) \leq \rho_F(\bar{\mu}_k, \mu(t_k)) + C\Delta t e^{C\Delta t}.$$

Substituting the latter expression into (3.19) yields

$$\|b_k - b(t, \mu(t))\|_{\mathbf{L}^\infty} \leq \|b\|_{\mathbf{BC}^{\alpha,1}} \left(\rho_F(\bar{\mu}_k, \mu(t_k)) + C\Delta t e^{C\Delta t} \right) + \|b\|_{\mathbf{BC}^{\alpha,1}} (\Delta t)^\alpha.$$

Bounds for (3.17) and (3.18) can be proved analogously. From the assumptions it holds that

$$\|(b, c, \beta)\|_{\mathbf{BC}^{\alpha,1}} = \|b\|_{\mathbf{BC}^{\alpha,1}} + \|c\|_{\mathbf{BC}^{\alpha,1}} + \sum_{p=1}^r \|\beta_p\|_{\mathbf{BC}^{\alpha,1}} < +\infty,$$

and as a consequence, we obtain

$$\|\bar{b}_k - b\|_{\overline{\mathbf{BC}}} + \|\bar{c}_k - c\|_{\overline{\mathbf{BC}}} + \sum_{p=1}^r \|\bar{\beta}_{p,k} - \beta_p\|_{\overline{\mathbf{BC}}} \leq \|(b, c, \beta)\|_{\mathbf{BC}^{\alpha,1}} \left[\rho_F(\bar{\mu}_k, \mu(t_k)) + C e^{CT} \Delta t + (\Delta t)^\alpha \right].$$

Using this inequality in (3.16) yields

$$\begin{aligned} \rho_F(\zeta(t_{k+1}), \mu(t_{k+1})) &\leq C \Delta t e^{C\Delta t} \left[\rho_F(\bar{\mu}_k, \mu(t_k)) + \Delta t + (\Delta t)^\alpha \right] \\ &\leq C \Delta t e^{C\Delta t} \rho_F(\bar{\mu}_k, \mu(t_k)) + C e^{CT} (\Delta t)^2 + C e^{CT} (\Delta t)^{1+\alpha}. \end{aligned}$$

Combining the inequality above with (3.15) and redefining C leads to

$$\begin{aligned} \rho_F(\nu(t_{k+1}), \mu(t_{k+1})) &\leq e^{C\Delta t} (1 + C\Delta t) \rho_F(\bar{\mu}_k, \mu(t_k)) + C(\Delta t)^2 + C(\Delta t)^{1+\alpha} \quad (3.20) \\ &\leq e^{2C\Delta t} \rho_F(\bar{\mu}_k, \mu(t_k)) + C(\Delta t)^2 + C(\Delta t)^{1+\alpha}. \end{aligned}$$

Finally, putting together (3.20) and (3.14), we conclude that

$$\rho_F(\bar{\mu}_k^2, \mu(t_{k+1})) \leq e^{2C\Delta t} \rho_F(\bar{\mu}_k, \mu(t_k)) + C(\Delta t)^2 + C(\Delta t)^{1+\alpha}. \quad (3.21)$$

Step 4: Adding the errors. Now, let $w = jn$, $v = (j-1)n$, $j \in \{1, \dots, \mathcal{K}\}$, that is, t_w and t_v are the time points in which the measure reconstruction occurs. Since for t_i such that $t_v < t_i < t_w$ it holds that $\bar{\mu}_i = \mathcal{R}(\bar{\mu}_{i-1}^2) = \bar{\mu}_{i-1}^2$, i.e., the measure reconstruction is not performed, the application of the discrete Gronwall's inequality to (3.21) yields

$$\rho_F(\bar{\mu}_w^2, \mu(t_w)) \leq e^{nC\Delta t} \rho_F(\bar{\mu}_v, \mu(t_v)) + C \frac{e^{nC\Delta t} - 1}{e^{C\Delta t} - 1} \left((\Delta t)^2 + (\Delta t)^{1+\alpha} \right).$$

There exists C^* depending only on T such that $e^{nC\Delta t} - 1 < nC^*\Delta t$, for each $n\Delta t \in [0, T]$. Therefore, we deduce

$$\frac{e^{nC\Delta t} - 1}{e^{C\Delta t} - 1} \leq \frac{nC^*\Delta t}{C\Delta t} = \frac{C^*}{C} n$$

and thus,

$$\rho_F(\bar{\mu}_w^2, \mu(t_w)) \leq e^{nC\Delta t} \rho_F(\bar{\mu}_v, \mu(t_v)) + nC \left((\Delta t)^2 + (\Delta t)^{1+\alpha} \right),$$

for some constant C . Combining this inequality with (3.11) in Step 2 of the proof yields

$$\rho_F(\bar{\mu}_w, \mu(t_w)) \leq e^{nC\Delta t} \rho_F(\bar{\mu}_v, \mu(t_v)) + nC \left((\Delta t)^2 + (\Delta t)^{1+\alpha} \right) + CE_R(\bar{M}).$$

Step 5: Final estimate for the auxiliary scheme. An analogous argument using the discrete Gronwall's inequality again results in the following estimate

$$\begin{aligned} \rho_F(\bar{\mu}_w, \mu(t_w)) &\leq e^{jnC\Delta t} \rho_F(\mathcal{R}(\mu_o), \mu_o) + C \frac{e^{jnC\Delta t} - 1}{e^{nC\Delta t} - 1} \left[n \left((\Delta t)^2 + (\Delta t)^{1+\alpha} \right) + E_R(\bar{M}) \right] \\ &\leq C e^{Ct_w} E_I(\bar{M}_o) + Cj \left[n \left((\Delta t)^2 + (\Delta t)^{1+\alpha} \right) + E_R(\bar{M}) \right] \\ &\leq C e^{Ct_w} E_I(\bar{M}_o) + C(jn\Delta t) \left(\Delta t + (\Delta t)^\alpha \right) + Cj E_R(\bar{M}) \quad (3.22) \end{aligned}$$

and since $jn\Delta t = t_w \leq T$ the assertion is proved.

Step 6: Full error estimate. The full error estimate (3.6) takes into account the error following from the numerical approximation of the auxiliary scheme (3.8)–(3.9). This additional source of error is nothing else than the error of the Euler method for ODE's. According to [8, (515.62)], the error committed is of order Δt when solving (3.8)–(3.9) using its Euler approximation (2.2)–(2.7). Therefore, the final estimate (3.22) holds. \square

Remark 3.23. *In this work, we have assumed that η is given as a sum of Dirac Deltas (1.2). If $\eta(t, \mu)(y)$ is not in such a form, one has to use a proper approximation by atomic measures in order to apply our scheme. One of the possibilities for this approximation is through the measure reconstruction described in Subsection 2.3. Assume that there exists a bounded interval K such that for all $(t, \mu) \in [0, T] \times \mathcal{M}^+(\mathbb{R}^+)$, we have*

$$\text{supp}(\eta(t, \mu)(y)) \subseteq K. \quad (3.24)$$

Fix $r \in \mathbb{N}$ and let $\{K_p\}_{p=1}^r$ be a family of intervals such that

$$\bigcup_{p=1}^r K_p = K, \quad K_i \cap K_j = \emptyset, \text{ for } i \neq j \quad \text{and} \quad |K_p| = \frac{|K|}{r}, \text{ where } p = 1, \dots, r.$$

Namely, we divide K into r disjoint intervals of equal length. Denote the center of each interval by $\bar{x}_p(y)$ and define

$$\beta_p(t, \mu)(y) = \int_{K_p} d(\eta(t, \mu)(y))(x). \quad (3.25)$$

The approximation of $\eta(t, \mu)(y)$ is thus given by

$$\sum_{p=1}^r \beta_p(t, \mu)(y) \delta_{x=\bar{x}_p(y)}. \quad (3.26)$$

If η is regular enough, then the assumptions on β_p and \bar{x}_p (3.1)–(3.4) are fulfilled for all r , and the numerical scheme we propose applies. In order to prove the convergence towards the solution of (1.1) with the parameter function η , we observe that the distance between η and its approximation (3.26) expressed in terms of the proper norm can be bounded by C/r , where C does not depend on t, μ and y due to (3.25)–(3.26). Thus, the most general version of the stability result in [13, Theorem 2.11] guarantees that if r tends to $+\infty$, then the numerical solution obtained for the approximated η converges towards a solution to (1.1) with the parameter function η . For all technical details, we refer to [13].

4 Simulation Results

This section is devoted to presenting results of numerical simulations for several test cases. In all examples presented in this paper, we used the 4-th order Runge-Kutta method for solving (2.2) and the explicit Euler scheme for solving (2.7), as described in Subsection 2.1. The error of the numerical solution with parameters $(\Delta t, \bar{M}_o, \bar{M})$ at time $T > 0$ is defined as

$$\text{Err}(T; \Delta t, \bar{M}_o, \bar{M}) := \rho(\mu(t_{\bar{k}}), \mu_{\bar{k}}), \quad (4.1)$$

with \bar{k} such that $\bar{k}\Delta t = T$. The order of the method q is given by

$$q := \lim_{\Delta t \rightarrow 0} \frac{\log(\text{Err}(T; 2\Delta t, 2\bar{M}_o, 2\bar{M})/\text{Err}(T; \Delta t, \bar{M}_o, \bar{M}))}{\log 2}. \quad (4.2)$$

We also define $\Delta x := |K|/\bar{M}_o$, where K is the minimal bounded closed interval containing the support of the initial measure. We will not distinguish between measures and their densities whenever the measures are absolutely continuous with respect to the Lebesgue measure.

4.1 Example 1 (McKendrick-von Foerster equation)

In this subsection, we validate the convergence result for our numerical scheme by means of the well-known McKendrick-von Foerster type equation [27]. This is a linear model describing the evolution of an size-structured population. We set

$$b(x) = 0.2(1 - x), \quad c(x) = 0.2, \quad \eta(y) = 2.4(y^2 - y^3)\delta_{x=0}, \quad \text{and} \quad \mu_o = \chi_{[0,1]}(x),$$

and solve (1.1) for $x \in [0, 1]$, see also [3]. The solution is stationary and then given by $\mu(t, x) = \chi_{[0,1]}(x)$. In Table 1, we present the relative error and the order of the scheme, where we used just one measure reconstruction in order to approximate the initial data. In Table 2, we present results for the scheme with the measure reconstruction performed at $t = 0, 1, \dots, 10$ and $\bar{M}_o = \bar{M}$. In all cases, we see that the convergence error approximates order one as $\Delta t \rightarrow 0$ as proven in Theorem 3.2 and Remark 3.7.

$\Delta t = \Delta x$	$\text{Err}(10, \Delta t, \bar{M}_o, \bar{M})$	q
$1.000000 \cdot 10^{-1}$	$1.2532 \cdot 10^{-2}$	-
$5.000000 \cdot 10^{-2}$	$5.0543 \cdot 10^{-3}$	1.31006
$2.500000 \cdot 10^{-2}$	$2.2225 \cdot 10^{-3}$	1.18533
$1.250000 \cdot 10^{-2}$	$1.0349 \cdot 10^{-4}$	1.10272
$6.250000 \cdot 10^{-3}$	$4.9832 \cdot 10^{-4}$	1.05431
$3.125000 \cdot 10^{-3}$	$2.4438 \cdot 10^{-4}$	1.02796
$1.562500 \cdot 10^{-3}$	$1.2099 \cdot 10^{-4}$	1.01419
$7.812500 \cdot 10^{-5}$	$6.0198 \cdot 10^{-5}$	1.00715
$3.906250 \cdot 10^{-4}$	$3.0024 \cdot 10^{-5}$	1.00359
$1.953125 \cdot 10^{-4}$	$1.4993 \cdot 10^{-5}$	1.00180
$9.765625 \cdot 10^{-5}$	$7.4920 \cdot 10^{-6}$	1.00090

Table 1: (Example 1) The relative error and order of the scheme at $T = 10$. One reconstruction performed at $t = 0$, $\bar{M} = \bar{M}_o$.

$\Delta t = \Delta x$	$\text{Err}(10, \Delta t, \bar{M}_o, \bar{M})$ (Fixed-location)	q	$\text{Err}(10, \Delta t, \bar{M}_o, \bar{M})$ (Fixed-equal mass)	q
$1.000000 \cdot 10^{-1}$	$3.4657 \cdot 10^{-1}$	-	$8.8838 \cdot 10^{-2}$	-
$5.000000 \cdot 10^{-2}$	$1.1670 \cdot 10^{-1}$	1.5703	$2.9437 \cdot 10^{-2}$	1.5935
$2.500000 \cdot 10^{-2}$	$3.4080 \cdot 10^{-2}$	1.7759	$1.0879 \cdot 10^{-2}$	1.4361
$1.250000 \cdot 10^{-2}$	$1.1863 \cdot 10^{-2}$	1.5224	$4.4725 \cdot 10^{-3}$	1.2824
$6.250000 \cdot 10^{-3}$	$3.6874 \cdot 10^{-3}$	1.6858	$1.9907 \cdot 10^{-3}$	1.1678
$3.125000 \cdot 10^{-3}$	$1.6866 \cdot 10^{-3}$	1.1285	$9.3351 \cdot 10^{-4}$	1.0926
$1.562500 \cdot 10^{-3}$	$6.8067 \cdot 10^{-4}$	1.3091	$4.5131 \cdot 10^{-4}$	1.0486
$7.812500 \cdot 10^{-4}$	$3.3212 \cdot 10^{-4}$	1.0352	$2.2178 \cdot 10^{-4}$	1.0250
$3.906250 \cdot 10^{-4}$	$1.5814 \cdot 10^{-4}$	1.0705	$1.0992 \cdot 10^{-4}$	1.0127
$1.953125 \cdot 10^{-4}$	$7.4507 \cdot 10^{-5}$	1.0858	$5.4719 \cdot 10^{-5}$	1.0063
$9.765625 \cdot 10^{-5}$	$3.6414 \cdot 10^{-5}$	1.0329	$2.7299 \cdot 10^{-5}$	1.0032

Table 2: (Example 1) The relative error and order of the scheme at $T = 10$. Reconstruction performed at $t = 0, 1, \dots, T$, $\bar{M} = \bar{M}_o$.

4.2 Example 2 (nonlinear growth term)

In this subsection, we present results for a model where b and η are equal to zero. Thus, we have conservation of the number of approximated Dirac Deltas, and consequently, there is no

need for reconstructions. We consider a nonlinear growth function c as in [17] of the form

$$c(t, \mu)(x) = a(x) - \int_{\mathbb{R}} \alpha(x, y) d\mu(y),$$

where

$$a(x) = A - x^2, \quad A > 0 \quad \text{and} \quad \alpha(x, y) = \frac{1}{1 + (x - y)^2}.$$

According to [13, Remark 2.3, Lemma 4.8], one can consider (1.1) on the whole \mathbb{R} , so that the result concerning well posedness still holds if all parameter functions verify the regularity properties (3.1)–(3.4) on the whole line. However, $a(x)$ is not globally Lipschitz on \mathbb{R} . Nevertheless, the global well-posedness theory still applies if we reduce to measures whose support lies in a fixed compact interval. Note that the support of the solution is invariant in time.

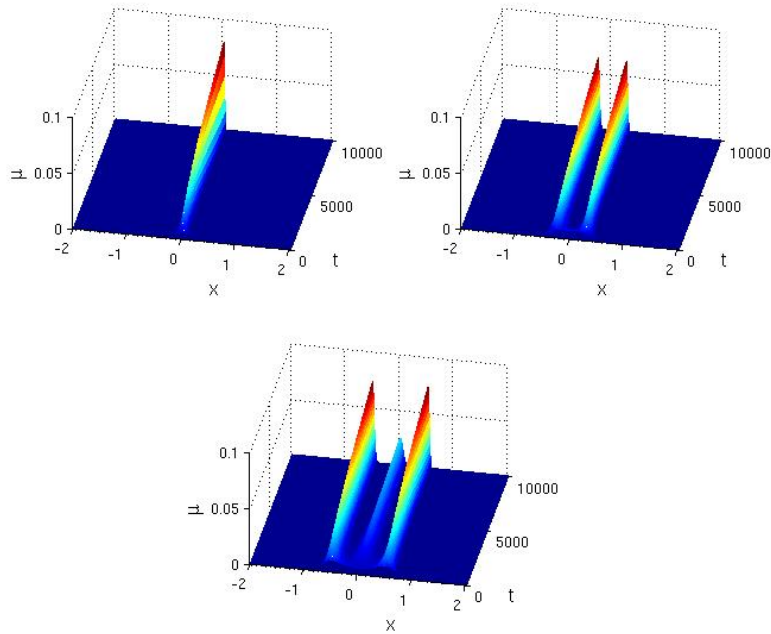


Figure 1: (Example 2) Long time behaviour of numerical solutions. The three subplots show the evolution of the numerical solution on the time interval $[0, 10000]$ for $A = 0.5, 1.5$ and 2.5 , respectively. For simulations, we set $\Delta t = 0.1$, $\bar{M}_o = 1000$ and $\mu_o = \sum_{i=1}^{\bar{M}_o} (1/\bar{M}_o) \delta_{x_o^i}$, where $x_o^i := -2 + (i - \frac{1}{2})/\bar{M}_o$. No measure reconstruction has been performed.

If $|x| > \sqrt{A}$, then the solution decreases exponentially to zero, since $\alpha(x, y) \geq 0$, for all $x, y \in \mathbb{R}$. This equation can describe a population structured with respect to the trait x , and then its asymptotic behaviour reflects the speciation process. Typically, after a long time period only a few traits are observable, since the rest of the population got extinct. Under some assumptions, there exists a linearly stable steady solution $\bar{\mu}$ being a sum of Dirac Deltas, which is shown in [17]. The number of Dirac measures depends on the parameter A and some stationary solutions are explicit. Figures 1 and 2 present the evolution and long time behaviour of solutions for different choices of the parameter A . These results are

consistent with the findings in [17]. In all cases, we assumed that initial data are given as a sum of uniformly distributed Dirac Deltas with the same mass.

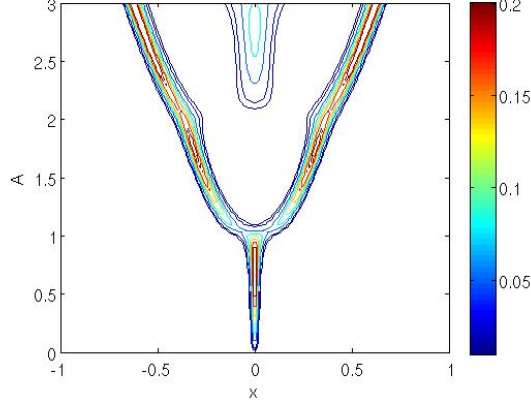


Figure 2: (Example 2) Stationary State as a function of $A > 0$. We show the numerical solution at time $t = 10000$ depending on the parameter $A \in [0, 3]$. For simulations, we set $\Delta t = 0.05$, $\bar{M}_o = 320$ and $\mu_o = \sum_{i=1}^{\bar{M}_o} (1/\bar{M}_o) \delta_{x_i^o}$, where $x_o^i := -2 + (i - \frac{1}{2})/\bar{M}_o$. No measure reconstruction has been performed.

4.3 Example 3 (size structure - equal fission)

In this subsection, we shall concentrate on a size-structured cell population model, in which a cell reproduces itself by fission into two equal parts. We assume that the cell divides after it has reached a minimal size $x_o > 0$. Therefore, there exists a minimum size whose value is $x_o/2$. Moreover, cells have to divide before they reach a maximal size, which is normalized to be equal to $x_{max} = 1$. Similarly as in [1], we set

$$x_o = \frac{1}{4}, \quad b(x) = 0.1(1-x), \quad c(x) = \beta(x), \quad \eta(t, \mu)(y) = 2\beta(y)\delta_{x=y/2}, \quad \text{and} \quad \mu_o(x) = (1-x)(x-x_o/2)^3,$$

where

$$\beta(y) = \begin{cases} 0, & \text{for } y \in (\mathbb{R}^+ \setminus [x_o, 1]), \\ \frac{b(y)\varphi(y)}{1 - \int_{x_o}^y \varphi(x) dx}, & \text{for } y \in [x_o, 1], \end{cases}$$

and

$$\varphi(y) = \begin{cases} \frac{160}{117} \left(-\frac{2}{3} + \frac{8}{3}y\right)^3, & \text{for } y \in [x_o, (x_o + 1)/2], \\ \frac{32}{117} \left(-20 + 40y + \frac{320}{3} \left(y - \frac{5}{8}\right)^2\right) + \frac{5120}{9} \left(y - \frac{5}{8}\right)^3 \left(\frac{8}{3}y - \frac{11}{3}\right), & \text{for } y \in ((x_o + 1)/2, 1]. \end{cases}$$

Figure 3 shows the long time behaviour of a numerical solution for a particular choice of parameters. We observe the convergence towards a stationary profile once normalized, since the mass grows exponentially in time, as discussed in [18, 1]. We remark that this structured population model cannot be discretized using the standard EBT method since particles divide

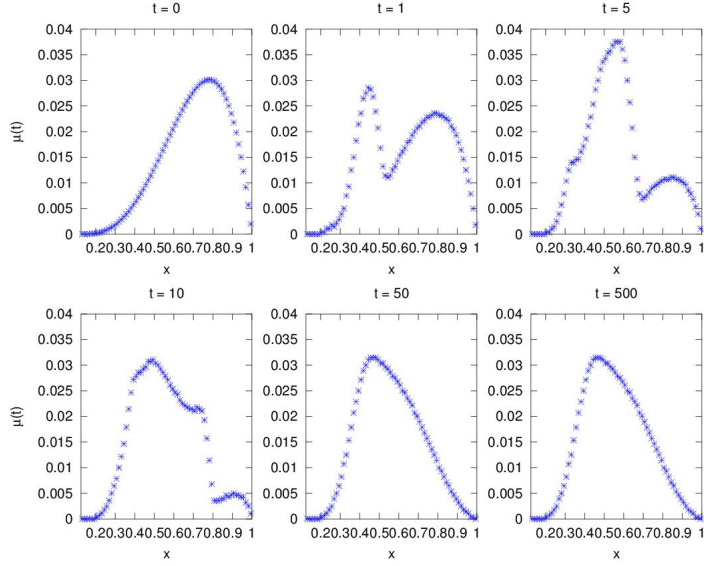


Figure 3: (Example 3) Numerical solution at $t = 0, 1, 5, 10, 50, 500$, calculated for $\Delta t = 0.0125$, $\bar{M}_o = \bar{M} = 2800$. Fixed-equal mass reconstruction has been performed every 4 time steps. We show the numerical solution after the fixed-location reconstruction with parameter $\bar{M} = 70$ and normalization.

at different sizes and the nonlocal term cannot be understood as a boundary condition. In order to keep the number of Dirac Deltas under control, we perform the reconstruction procedure as discussed in Subsection 2.3. Let us point out that the convergence towards normalized stationary states for similar models in the framework of Lebesgue spaces has been proved in [29, 26, 9, 4]. Finding the properties of these stationary states numerically is a relevant question that will be discussed elsewhere.

4.4 Example 4 (selection-mutation)

The last test case concerns a simple selection-mutation model in which the population is structured with respect to an evolutionary trait as in [10]. We assume that $x \in [0, 1]$ and set the parameters as

$$b(x) = 0, \quad c(\mu)(x) = -(1 - \varepsilon)B(x) + m(\mu), \quad \text{and} \quad \eta(y) = \varepsilon \sum_{p=1}^r B(y)\beta_p(y)\delta_{x=\bar{x}_p(y)}.$$

Here, $B(x)$ represents the trait specific birth rate, $m(\mu)$ is the death rate depending on the population distribution, and β_p represents the mutation density probability, i.e., the probability that a parent with trait y has a newborn with trait $\bar{x}_p(y)$. Finally, the parameter ε is the mutation rate, and thus there are two parts in the right hand side, those that are a faithful reproduction of their parents and those that mutate, slightly with high probability, their trait.

Let us point out that the mutation term in this model is an approximation in the sense

of Remark 3.23 of a continuous nonlocal term of the form

$$\int_0^1 B(y)\beta(x, y) \, d\mu(y) \quad \text{with} \quad \int_0^1 \beta(x, y) \, dx = 1,$$

and, in practice we can assume that has a Gaussian shape concentrated around the diagonal $x = y$. The approximated nonlocal term is constructed by substituting the mutation probability density $\beta(x, y)$ at each y by an approximation with r Delta Dirac points $\{\bar{x}_p(y)\}_{p=1}^r$ leading to the form of $\eta(y)$ above. More precisely, the approximated $\eta(y)$ is defined by duality on test functions $\varphi \in \mathbf{C}_0(\mathbb{R}^+)$ functions as

$$\begin{aligned} \int_{\mathbb{R}^+} \int_{\mathbb{R}^+} \varphi(t, x) B(y)\beta(x, y) \, dx \, d\mu(y) &\approx \sum_{p=1}^r \int_{\mathbb{R}^+} B(y)\beta_p(y)\varphi(\bar{x}_p(y)) \, d\mu(y) \\ &= \int_{\mathbb{R}^+} \int_{\mathbb{R}^+} \varphi(t, x) [d\eta(t, \mu)(y)](x) \, d\mu(y). \end{aligned}$$

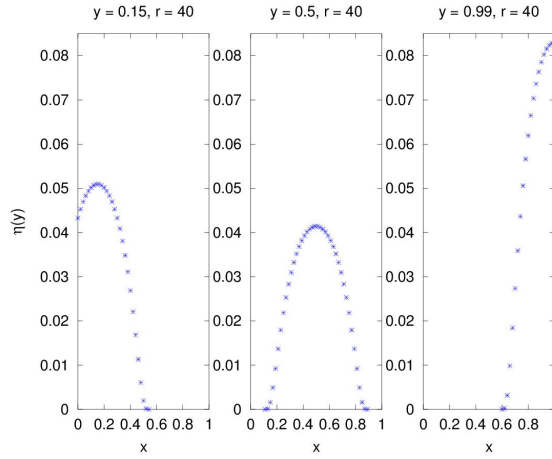


Figure 4: (Example 4) The subplots show the function $\eta(y)$ for $y = 0.15$, $y = 0.5$ and $y = 0.99$, respectively, and parameters $r = 40$, $a = 0.4$.

In our simulations and based on the previous considerations, we consider $B(x) = x(1 - x)$, the death rate is assumed to depend increasingly on the total population with a saturation of the form $m(\mu) = 1 - \exp\{-\int_0^1 d\mu\}$, and the approximation of the mutation kernel is chosen with $r = 10$,

$$\bar{x}_p(y) = \begin{cases} (y - a) + \frac{a}{r} (2p - 1), & \text{if } 0 \leq (y - a) + \frac{a}{r} (2p - 1) \leq 1, \\ 0, & \text{otherwise,} \end{cases}$$

and

$$\beta_p(y) = \frac{\check{\beta}_p(y)}{\sum_{p=1}^r \check{\beta}_p(y)}, \quad \text{where } \check{\beta}_p(y) = \begin{cases} \exp\left(-\frac{a^2}{a^2 - (\bar{x}_p(y) - y)^2}\right), & \text{if } p \text{ is s.t. } 0 \leq \bar{x}_p(y) \leq 1, \\ 0, & \text{otherwise.} \end{cases}$$

The parameter a is related to the mutation strength in the sense that a distance between a parent and its offspring is not greater than a , set in our simulations to $a = 0.4$.

Figure 5 shows the convergence towards stationary states for different values of the mutation rate ε . We observe that the stabilization rate depends on ε , being slower as ε gets smaller and smaller. The existence of these stationary states with the full mutation kernel η was proved in [10] without information about their stability.

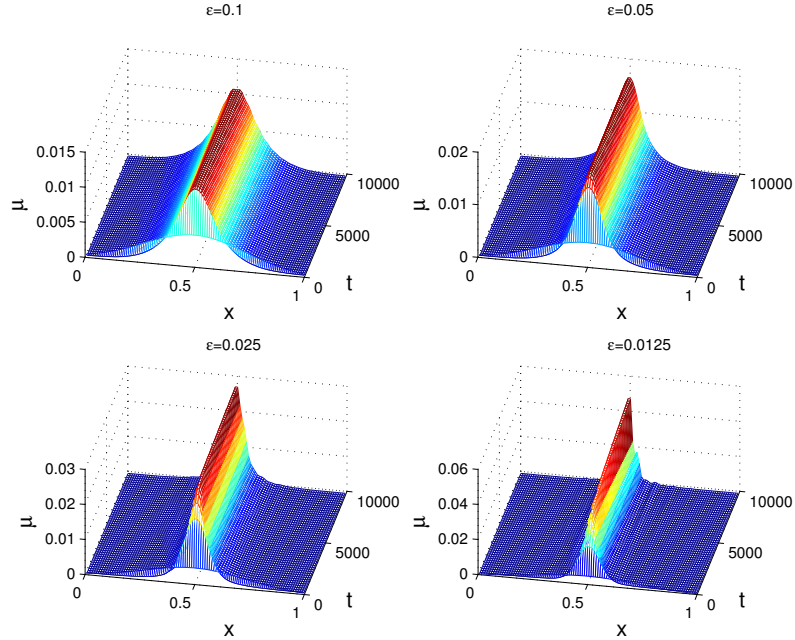


Figure 5: (Example 4) Long time behaviour of numerical solutions. The plots show the evolution of a numerical solution on the time interval $[0, 2000]$ for $\varepsilon = 0.1, 0.05, 0.025,$ and $0.0125,$ respectively. For simulations, we set $\Delta t = 0.025,$ $\bar{M}_o = \bar{M} = 100,$ and $\mu_o = \sum_{i=1}^{\bar{M}_o} (1/\bar{M}_o)\delta_{x_o^i},$ where $x_o^i := (i - \frac{1}{2})/\bar{M}_o.$ Fixed location reconstruction has been performed every 2 time steps.

Acknowledgments

JAC acknowledges support from the Royal Society by a Wolfson Research Merit Award and by the Engineering and Physical Sciences Research Council grant with references EP/K008404/1. JAC was partially supported by the project MTM2011-27739-C04-02 DGI (Spain) and 2009-SGR-345 from AGAUR-Generalitat de Catalunya. PG is the coordinator and AU is a Ph.D student in the International Ph.D. Projects Programme of Foundation for Polish Science operated within the Innovative Economy Operational Programme 2007-2013 (Ph.D. Programme: Mathematical Methods in Natural Sciences). PG is supported by the grant of National Science Centre no 6085/B/H03/2011/40. AU is supported by the grant of National Science Centre no 2012/05/N/ST1/03132.

References

- [1] L. M. Abia, O. Angulo, and J. C. Lopez-Marcos. Numerical schemes for a size-structured cell population model with equal fission. *Mathematical and Computer Modelling*, 50:653–

664, 2009.

- [2] L. Ambrosio, N. Gigli, and G. Savaré. *Gradient flows in metric spaces and in the space of probability measures*. Lectures in Mathematics ETH Zürich. Birkhäuser Verlag, Basel, 2005.
- [3] O. Angulo and J. C. Lopez-Marcos. Numerical schemes for size-structured population equations. *Mathematical Biosciences*, 157:169–188, 1999.
- [4] D. Balagué, J. A. Cañizo, and P. Gabriel. Fine asymptotics of profiles and relaxation to equilibrium for growth-fragmentation equations with variable drift rates. *Kin. Rel. Mod.*, 6(22):219–243, 2013.
- [5] C. K. Birdsall and Langdon A. B. *Plasma Physics Via Computer Simulation*. McGraw-Hill, New York, 1985.
- [6] A. Brannstrom, L. Carlsson, and D. Simpson. On the convergence of the escalator boxcar train. *arXiv:1210.1444v1*.
- [7] C. J. Briggs, R. M. Nisbet, W. W. Murdoch, T. R. Collier, and J. A. J. Metz. Dynamical effects of host-feeding in parasitoids. *Journal of Animal Ecology*, 64:403 – 416.
- [8] J. C. Butcher. *Numerical methods for ordinary differential equations*. John Wiley & Sons Ltd., Chichester, second edition, 2008.
- [9] M. J. Cáceres, J. A. Cañizo, and S. Mischler. Rate of convergence to an asymptotic profile for the self-similar fragmentation and growth-fragmentation equations. *J. Math. Pures Appl. (9)*, 96(4):334–362, 2011.
- [10] A. Calsina, S. Cuadrado, L. Desvillettes, and G. Raoul. Asymptotics of steady states of a selection-mutation equation for small mutation rate. *to appear in Proc. Roy. Soc. A*, 2013.
- [11] J. A. Cañizo, J. A. Carrillo, and S. Cuadrado. Measure solutions for some models in population dynamics. *Acta Appl. Math.*, 123:141–156, 2013.
- [12] J. A. Cañizo, J. A. Carrillo, and J. Rosado. A well-posedness theory in measures for some kinetic models of collective motion. *Math. Models Methods Appl. Sci.*, 21(3):515–539, 2011.
- [13] J. A. Carrillo, R. Colombo, P. Gwiazda, and A. Ulikowska. Structured populations, cell growth and measure valued balance laws. *J. Differential Equations*, 252(4):3245–3277, 2012.
- [14] R. M. Colombo and G. Guerra. Differential equations in metric spaces with applications. *Discrete Contin. Dyn. Syst.*, 23(3):733–753, 2009.
- [15] G.-H. Cottet and P.-A. Raviart. Particle methods for the one-dimensional Vlasov-Poisson equations. *SIAM J. Numer. Anal.*, 21(1):52–76, 1984.
- [16] A. M. de Roos. Numerical methods for structured population models: the escalator boxcar train. *Numer. Methods Partial Differential Equations*, 4(3):173–195, 1988.

- [17] L. Desvillettes, P.E. Jabin, S. Mischler, and G. Raoul. On selection dynamics for continuous structured populations. *Commun. Math. Sci.*, 6(3):729–747, 2008.
- [18] O. Diekmann, H. J. A. M. Heijmans, and H. R. Thieme. On the stability of the cell size distribution. *J. Math. Biol.*, 19(2):227–248, 1984.
- [19] M. R. D’Orsogna, Y. Chuang, A. L. Bertozzi, and L. Chayes. Self-propelled particles with soft-core interactions: patterns, stability and collapse. *Phys. Rev. Lett.*, 96(104302), 2006.
- [20] K. Ganguly and H. D. Victory, Jr. On the convergence of particle methods for multidimensional Vlasov-Poisson systems. *SIAM J. Numer. Anal.*, 26(2):249–288, 1989.
- [21] R. Goetz, N. Hritonenko, A. Xabadia, and Y. Yatsenko. *Using the escalator boxcar train to determine the optimal management of a size-distributed forest when carbon sequestration is taken into account*. Large-Scale Scientific Computing, vol. 4818 of Lectures Notes in Computer Science. Springer, Berlin, 2008.
- [22] J. Goodman, T. Y. Hou, and J. Lowengrub. Convergence of the point vortex method for the 2-D Euler equations. *Comm. Pure Appl. Math.*, 43(3):415–430, 1990.
- [23] P. Gwiazda, T. Lorenz, and A. Marciniak-Czochra. A nonlinear structured population model: Lipschitz continuity of measure-valued solutions with respect to model ingredients. *J. Differential Equations*, 248(11):2703–2735, 2010.
- [24] P. Gwiazda and A. Marciniak-Czochra. Structured population equations in metric spaces. *J. Hyperbolic Differ. Equ.*, 7(4):733–773, 2010.
- [25] T. Kolokonikov, H. Sun, D. Uminsky, and A. L. Bertozzi. Stability of ring patterns arising from 2d particle interactions. *Physical Review E*, 84(1):015203, 2011.
- [26] P. Laurençot and B. Perthame. Exponential decay for the growth-fragmentation/cell-division equation. *Commun. Math. Sci.*, 7(2):503–510, 2009.
- [27] A. G. McKendrick. Applications of mathematics to medical problems. *Proc. Edinburgh Math. Soc.*, 44:98–130, 1926.
- [28] L. Persson, K. Leonardsson, A.M. de Roos, M. Gyllenberg, and B Christensen. Ontogenetic scaling of foraging rates and the dynamics of a size-structured consumer-resource model. *Theoretical Population Biology*, 54:270–293, 1998.
- [29] B. Perthame and L. Ryzhik. Exponential decay for the fragmentation or cell-division equation. *J. Differential Equations*, 210(1):155–177, 2005.
- [30] B. Piccoli and F. Rossi. Generalized wasserstein distance and its application to transport equations with source. *arXiv:1206.3219*, 2012.
- [31] B. Piccoli and A. Tosin. Time-evolving measures and macroscopic modeling of pedestrian flow. *Arch. Ration. Mech. Anal.*, 199(3):707–738, 2011.
- [32] C. Villani. *Topics in Optimal Transportation*, volume 58 of (*Graduate Studies in Mathematics*). American Mathematical Society, 2008.

- [33] M. Westdickenberg and J. Wilkening. Variational particle schemes for the porous medium equation and for the system of isentropic Euler equations. *M2AN Math. Model. Numer. Anal.*, 44(1):133–166, 2010.
- [34] A. Xabadia and R.U. Goetz. The optimal selective logging regime and the faustmann formula. *Journal of Forest Economics*, 16:63–82, 2010.